SARS-CoV-2 induces inflammasome-dependent pyroptosis and downmodulation of HLA-DR in human monocytes

André C. Ferreira[1,2,10#*], Vinicius Cardoso Soares[1,9#], Isaclaudia G. de Azevedo-Quintanilha[1], Suelen da Silva Gomes Dias[1], Natalia Fintelman-Rodrigues[1,10], Carolina Q. Sacramento[1,10], Mayara Mattos[1,10], Caroline S. de Freitas[1,10], Jairo R. Temerozo[3,4], Lívia Teixeira[1], Eugenio Damaceno Hottz[1,5], Ester A Barreto[1], Camila R. R. Pão[1], Lohanna Palhinha[1], Milene Miranda[6], Dumith Chequer Bou-Habib[3,4], Fernando A. Bozza[7,8], Patrícia T. Bozza[1] , Thiago Moreno L. Souza[1,10*]

1 – Laboratório de Imunofarmacologia, Instituto Oswaldo Cruz (IOC), Fundação Oswaldo Cruz (Fiocruz), Rio de Janeiro, RJ, Brazil.

2 – Laboratório de Pesquisa Pré-clínica - Universidade Iguaçu, Nova Iguaçu, RJ, Brazil.

3 – Laboratório de Pesquisas sobre o Timo, IOC, Fiocruz, Rio de Janeiro, RJ, Brazil.

4 – National Institute for Science and Technology on Neuroimmunomodulation, Oswaldo Cruz Institute, Fiocruz, Rio de Janeiro, RJ, Brazil.

5 – Laboratório de Imunotrombose, Departamento de Bioquímica, Universidade Federal de Juiz de Fora, Juiz de Fora, MG, Brazil.

6 – Laboratório de Vírus Respiratório e do Sarampo, IOC, Fiocruz, Rio de Janeiro, RJ, Brazil.

7 – Instituto Nacional de Infectologia Evandro Chagas, Fiocruz, Rio de Janeiro, RJ, Brazil.

8 – Instituto D'or de Pesquisa e Ensino, Rio de Janeiro, RJ, Brazil.

9 - Program of Immunology and Inflammation, Federal University of Rio de Janeiro, UFRJ, Rio de Janeiro, RJ, Brazil.

10 - Centro De Desenvolvimento Tecnológico Em Saúde (CDTS), Fiocruz, Rio de Janeiro, Brasil.

# These authors contributed equally to this work

* corresponding author

Abstract

Infection by the severe acute respiratory syndrome coronavirus 2 (SARS-CoV-2) has been associated with leukopenia and uncontrolled inflammatory response in critically ill patients. A better comprehension of SARS-CoV-2-induced monocyte death is essential for the identification of therapies capable to control the hyper-inflammation and reduce viral replication in patients with COVID-19. Here, we show that SARS-CoV-2 induces inflammasome activation and cell death by pyroptosis in human monocytes, experimentally infected and from patients under intensive care. Pyroptosis was dependent on caspase-1 engagement, prior to IL-1ß production and inflammatory cell death. Monocytes exposed to SARS-CoV-2 downregulate HLA-DR, suggesting a potential limitation to orchestrate the immune response. Our results originally describe mechanisms by which monocytes, a central cellular component recruited from peripheral blood to respiratory tract, succumb to control severe 2019 coronavirus disease (COVID-19).

Author summary

Since its emergence in China in late 2019, severe acute respiratory syndrome coronavirus 2 (SARS-CoV-2) has caused thousands of deaths worldwide. Currently, the number of individuals infected with SARS-CoV-2 and in need of antiviral, anti-inflammatory, anticoagulant and more invasive treatments has overwhelmed the health systems worldwide. In our study, we found that SARS-CoV-2 is capable of inducing inflammatory cell death in human monocytes, one of the main cell types responsible for anti-SARS-CoV-2 immune response. As a consequence of this intracellular inflammatory mechanism (inflammasome engagement), an exacerbated production of inflammatory mediators occurs. The infection also decreases the expression of HLA-DR in monocytes, a molecule related to the orchestration of the immune response in case of viral infections. We also demonstrated that the HIV-1 protease inhibitor, atazanavir (ATV), prevented the uncontrolled inflammatory response, cell death and reduction in HLA-DR expression in SARS-CoV-2-infected monocytes. Our study provides relevant information on the effects of SARS-CoV-2 infection on human monocytes, as well as on the effect of ATV in preventing these pathological effects on the host.

Introduction

Severe acute respiratory coronavirus 2 (SARS-CoV-2), the etiological agent of the 2019 coronavirus disease (COVID-19), emerged in China, causing a major public health burden in decades. Patients with COVID-19 may develop an asymptomatic or mild disease or be affected by the life threatening acute respiratory distress syndrome (ARDS), which is characterized by elevated serum levels of proinflammatory mediators, the cytokine storm (1–3). In the respiratory tract of patients with severe COVID-19, monocytes/macrophages may be the main source of uncontrolled levels of the pro-inflammatory mediators TNF-α and IL-6 (4). Plasmatic levels of IL-6 have been associated with mortality, intensive care admission and hospitalization, representing a poor prognostic factor for COVID-19 (5). The uncontrolled inflammation promoted by SARS-CoV-2 in severe COVID-19 is not acute, it negatively associates with viral loads in nasopharyngeal swabs and represents an important event from 7 to 10 days after onset of illness (6,7). The SARS-CoV-2-induced cytokine storm associates with intense cell death (8,9).

There are various mechanisms involved in cell death, which are differently engaged from development to responses to infection (10). For certain diseases, such as COVID-19, in which the immunopathogenesis mechanisms associate with poor clinical outcomes, controlling the way cells collapse to infection is vital for the host (10). For example, cell death from necrosis, which can occur from necroptosis to pyroptosis, tends to exacerbate inflammation due to the rupture of the cellular plasma membrane. Pyroptosis, in particular, begins with the activation of the inflammasome, an intracellular structure that involves several intracellular molecules such as caspase-1(10,11), leads to leakage of the cytoplasmic content, favors inflammatory infiltrate (11) and amplifies of the inflammatory response (12). These mechanisms of cell death contrasts with apoptosis, a more controlled process that maintain the host's homeostasis.

In severe COVID-19, the cytokine storm associates with high levels of tissue insult, judged by increased levels lactate dehydrogenase (LDH) and D-dimer in the plasma (6–8). Moreover, high LDH levels and leukopenia in severe COVID-19 points out that white cells loses the integrity of plasma membrane (6–8). Among these cells,

96 monocytes should orchestrate the equilibrium between innate and adaptative immune
97 responses, which may be presumably affected during cytokine storm. Indeed, severe
98 immune dysregulation with low antigen presenting capacity is evidenced by reduced
99 expression of HLA-DR in monocytes during COVID-19, which is strongly associated
100 with severe respiratory failure (4).

101 The leukopenia of patients with severe COVID-19 seem to precede the cytokine
102 storm (13–18). Moreover, in other virus-induced cytokine storm episodes in the
103 respiratory tract, such as induced by influenza A virus, monocytes and macrophages are
104 severely affected (13). Thus, we hypothesized that the monocyte cell death induced by
105 SARS-COV-2 exacerbates the production of inflammatory cytokines, as well as impairs
106 the immune balance in the hosts. In fact, we found that SARS-CoV-2 triggers the
107 activation of the inflammasome, leading to pyroptosis in human monocytes, by
108 experimental or natural infection. Pyroptosis was dependent on caspase-1 engagement,
109 prior to IL-1ß production and dysregulation of cytokine release. Monocytes that survive
110 after SARS-CoV-2 challenge downregulate HLA-DR, being less likely to properly
111 orchestrate the immune response. Finally, we show that the reproposed antiviral drug
112 atazanavir (ATV) could block this deleterious loop in favor of the host.

113 Material and Methods

114 Reagents

115 Atazanavir (ATV) and Ribavirin were received as donations from Instituto de
116 Tecnologia de Fármacos (Farmanguinhos, Fiocruz). The antiviral Lopinavir/ritonavir
117 (4:1 proportion) was pruchased from AbbVie (Ludwingshafen, Germany). ELISA assays
118 were purchased from R&D Bioscience. Lipopolysacchadides - LPS, adenosine
119 triphosphate (ATP), the specific inhibitor of caspase-1 (AC-YVAD-CMK), pan-caspase
120 inhibitor (ZVAD-FMK), RIPK1 (Necrostatin-1 – Nec-1) and IL-1 receptor (IL-1RA)
121 were all purchased from Sigma-Aldrich (St. Louis, MO, USA). All small molecule
122 inhibitors were dissolved in 100 % dimethylsulfoxide (DMSO) and subsequently diluted
123 at least 10^4-fold in culture or reaction medium before each assay. The final DMSO
124 concentrations showed no cytotoxicity. The materials for cell culture were purchased
125 from Thermo Scientific Life Sciences (Grand Island, NY), unless otherwise mentioned.

126

127 **Cells and Virus**

128 African green monkey kidney (Vero, subtype E6) cells were cultured in DMEM
129 high glucose supplemented with 10 % fetal bovine serum (FBS; HyClone, Logan, Utah)
130 and 100 U/mL penicillin, and 100 µg/mL streptomycin (P/S). Vero cells were incubated
131 at 37°C in 5 % CO_2 atmosphere.

132 Human primary monocytes were obtained through plastic adherence of peripheral
133 blood mononuclear cells (PBMCs), which were obtained from buffy coat preparations of
134 healthy donors by density gradient centrifugation (Ficoll-Paque, GE Healthcare). In brief,
135 PBMCs (2.0 x 10^6 cells) were plated onto 48-well plates (NalgeNunc) in RPMI-1640
136 without serum for 2 to 4 h; then, non-adherent cells were removed by washing and the
137 remaining monocytes were maintained in DMEM with 5% human serum (HS; Millipore)
138 and penicillin/streptomycin.

139 SARS-CoV-2 was isolated and expanded on Vero E6 cells from a nasopharyngeal
140 swab of a confirmed case from Rio de Janeiro, Brazil. Experiments were performed after
141 one passage in cell culture, when Vero E6 cells with DMEM plus 2% FBS in 150 cm^2
142 flasks were incubated at 37 °C in 5 % CO_2 atmosphere. Cytopathic effect was observed
143 daily and peaked 4 to 5 days after infection. All procedures related to virus culture were
144 handled at biosafety level 3 (BSL3) multiuser facility, according to WHO guidelines.
145 Virus titers were determined as the tissue culture infectious dose at 50% (TCID50/mL).
146 Virus stocks were kept in -80 °C ultralow freezers. The virus strain was sequenced to
147 confirm the virus identity and its complete genome is publicly deposited (GenBank
148 accession no. MT710714).

149 **Yield-reduction assay**

150 Human primary monocytes were infected with multiplicity of infection (MOI) of
151 0.01 at density of 2-8 x 10^5 cells/well in 48-well culture plates, depending on the total cell
152 number from each donor. After 1 h at 37 °C, cells were washed, and various
153 concentrations of compounds were added in DMEM with 2% FBS. After 48 h, the

154 supernatants were harvested and virus replication was quantified by real time RT- PCR
155 and infectious titers by TCID50/mL.

156 **Virus titration**

157 Monolayers of Vero cells (2 x 10^4 cell/well) in 96-well culture plates were infected
158 with log- based dilutions of the supernatants containing SARS-CoV-2 for 1 h at 37°C.
159 The cells were washed and fresh medium with 2% FBS was added. After 3 to 5 days, the
160 cytopathic effects were scored in at least 10 replicates per dilution by independent readers,
161 who were blind with respect to source of the supernatant. Reed and Muench scoring
162 method was employed to determine TCID50/mL.

163 **Flow cytometer analysis**

164 For flow cytometry analysis, monocytes were diluted in labelling buffer (10^6
165 cells/mL). Then, 100 µL of cell samples were marked with 5 µL of AnnexinV and PI for
166 15 minutes for cell death evaluation. Around 10,000 gated events were acquired using
167 FACSCalibur and the analysis was performed using the CellQuest software. Monocytes
168 were gated through cell size (foward light scatter, FSC) and granularity (side light scatter,
169 SSC) analysis.

170 Human monocytes were stained for caspase-1 activity with FAM-YVAD-FMK
171 (fluorescent-labeled inhibitor of caspase-1 [FLICA] and FAM-FLICA Caspase-3/7
172 activity or HLA-DR APC.H7 or IgG APC.H7. Caspase-1 and caspase-3/7 activity was
173 determined via flow cytometry (FACSCalibur) by detecting FLICA fluorescence and
174 expression of HLA-DR as mean fluorescence intensity (MFI) value for each sample.
175 Acquisition of data was set to count a total of 10,000 events, and the FLOWJO software
176 package was used to analyze the data.

177 **Microscopic analysis**

178 Human primary monocytes were plated on glass coverslips at density of 2-8 x 10^5
179 cells/well in 48-well plates. Infection was performed for 2 h at 37 °C and then fresh
180 medium with 2% FBS was added. After 24 h, the cells were washed with Binding buffer
181 and stained with PI (0.5 µg/mL) for 5 minutes. Next, the cells were fixed with 3.7%
182 formaldehyde for 30 minutes at room temperature. The nuclei were stained with DAPI

183 (1µg/mL) for 5 min and the coverslips were mounted using an antifade mounting medium
184 (VECTASHIELD). Fluorescence was analyzed by fluorescence microscopy with an x100
185 objective lens (Olympus, Tokyo, Japan).

186 **Measurements Inflammatory Mediators and cell death marker**

187 The levels of IL-1ß, TNF-α, IL-6, IL-8 and LDH were quantified in the culture
188 supernatants from infected and uninfected monocytes using ELISA kits, according to the
189 manufacturer's intructions (R&D System).

190 Extracellular lactate dehydrogenase (LDH) was quantified using Doles® kit
191 according to manufacturer's instructions. In brief, cell culture supernatants were
192 centrifuged at 5,000 rpm for 1 minute, to remove cellular debris, and then 25 µL were
193 placed into 96-well plates and incubated with 5 µL of ferric alum and 100 µL of LDH
194 substrate for 3 minutes at 37 ºC. Nicotinamide adenine dinucleotide (NAD, oxidized
195 form) was added followed by the addition of a stabilizing solution. After 10 minutes, the
196 reaction was read in a spectrophotometer at 492 nm.

197 **Western blot assay**

198 Cellular extracts of $1x10^6$ cells were homogenized in the RIPA lysis buffer in the
199 presence of proteinase inhibitor cocktail (Roche), and the protein levels were measured
200 by BCA protein assay kit. A total of 20 µg of protein was loaded onto a 10% sodium
201 dodecyl sulfate polyacrylamide gel (SDS-PAGE) for separation by electrophoresis and
202 the protein bands were then transferred to a polyvinylidene difluoride membranes
203 (ImmobilonP-SQ, Millipore). The membranes were blocked with 5 % albumin diluted in
204 Tris-buffered saline containing 0.05 % of Tween 20 for 2 hours at room temperature and
205 incubated with the specific primary antibodies (Cell Signaling Technology), to detect pro-
206 caspase-1 and cleaved-caspase-1, after overnight incubation at 4 °C. After washing,
207 membranes were incubated with secondary antibodies (IRDye® 800CW Goat-anti-
208 Mouse and IRDye® 680LT Goat anti-Rabbit IgG Antibody, LI-COR, Lincoln) for 30
209 minutes at RT. The protein bands were visualized by digital fluorescence
210 (Odyssey® CLx Imaging System), and protein density was analyzed by the ImageJ
211 software. All the data were normalized by β-actin expression quantification.

212

213 **Human subjects.**

214 We prospectively enrolled severe COVID19 RT-PCR-confirmed cases, as well as
215 SARS-CoV-2-negative healthy controls. Blood samples were obtained from 12 patients
216 with severe COVID-19 within 72 hours from intensive care unit (ICU) admission in two
217 reference centers (Instituto Estadual do Cérebro Paulo Niemeyer and Hospital Copa Star,
218 Rio de Janeiro, Brazil). Severe COVID-19 was defined as critically ill patients presenting
219 viral pneumonia on computed tomography scan and in mechanical ventilation. All
220 patients had SARSCoV-2 confirmed diagnostic through RT-PCR of nasal swab or
221 tracheal aspirates. Peripheral vein blood was also collected from 8 SARS-CoV-2-negative
222 healthy control participants as tested by RT-PCR on the day of blood sampling. The
223 characteristics of severe (n = 12), and control (n = 8) participants are presented in Table
224 1. Severe COVID-19 patients usually present older age and higher prevalence of
225 comorbidities as obesity, cardiovascular diseases and diabetes as in previously reported
226 patient cohorts. In the present study, the SARS-CoV-2-negative control group was
227 designed to include subjects of older age and chronic non-communicable diseases, so it
228 is matched with critically ill COVID-19 patients (Table 1). Patients with acute respiratory
229 distress syndrome (ARDS) were managed with neuromuscular blockade and a protective
230 ventilation strategy that included low tidal volume (6 mL/kg of predicted body weight)
231 and limited driving pressure (less than 16 cmH2O) as well as optimal PEEP calculated
232 based on the best lung compliance and PaO_2/FiO_2 ratio. In those with severe ARDS and
233 PaO_2/FiO_2 ratio below 150 despite optimal ventilatory settings, prone position was
234 initiated. Our management protocol included antithrombotic prophylaxis with enoxaparin
235 40 to 60 mg per day. Patients did not receive routine steroids, antivirals or other anti-
236 inflammatory or anti-platelet drugs. The SARS-CoV-2- negative control participants
237 were not under anti-inflammatory or anti-platelet drugs for at least two weeks. All clinical
238 information were prospectively collected using a standardized form - ISARIC/WHO
239 Clinical Characterization Protocol for Severe Emerging Infections (CCPBR).

240 **Ethics statement.**

241 Experimental procedures involving human cells from healthy donors were
242 performed with samples obtained after written informed consent and were approved by
243 the Institutional Review Board (IRB) of the Oswaldo Cruz Foundation/Fiocruz (Rio de
244 Janeiro, RJ, Brazil) under the number 397-07. The National Review Board approved the

245 study protocol (CONEP 30650420.4.1001.0008), and informed consent was obtained
246 from all participants or patients' representatives.

247 **Statistical analysis**

248 The assays were performed in blinded way. They were performed by one
249 professional, codified and read by another fellow. All experiments were carried out at
250 least three independent times, including a minimum of two technical replicates in each
251 assay. The equations to fit the best curve were generated based on R^2 values ≥ 0.9.
252 Student's T-test was used to access statistically significant P values <0.05.

253 ## Results

254 **SARS-CoV-2 promotes pyroptosis in human monocytes**

255 To characterize the mechanism by which SARS-CoV-2 triggers monocyte death,
256 human primary monocytes were infected with SARS-CoV-2 or treated with LPS+ATP.
257 Next, cell death was analyzed by quantifying the LDH activity in the culture supernatant,
258 and by AnnexinV/propidium iodide (PI) cell labeling through for flow cytometry and
259 fluorescence microscopy. As shown in Figure 1A, SARS-CoV-2 increased LDH levels
260 similarly to the positive control, LPS+ATP (Figure 1A). Flow cytometry and fluorescence
261 microscopy images demonstrated higher percentages of PI^+ cells in the infected cultures,
262 as well as a significant increase in mean fluorescence intensity (MFI). Both, LDH leak
263 and PI labeling characterize cell membrane disruption in human monocytes after SARS-
264 CoV-2 infection (Figure 1B-E). These data suggest that SARS-CoV-2 infection can
265 induce cell death characterized by loss of plasma membrane integrity suggestive of
266 pyroptosis cell death.

267 **SARS-CoV-2 induces pyroptosis in monocytes through inflammasome activation**

268 To gain insights on the mechanisms of monocyte cell death in SARS-CoV-2
269 infection, we accessed caspase-1 activation - a key events that require inflammasome's
270 proteolytic activity. Cells stimulated with LPS+ATP were used as a positive control of
271 inflammasome activation. We observed that SARS-CoV-2 induced pro-caspase-1
272 cleavage, similarly to positive control (Figure 2A and 2B). To confirm these results, cells
273 were labeled with FAM-YVAD-FLICA (as an indicative of caspase-1 activation) and

274 analyzed by flow cytometry. We found that SARS-CoV-2 infection induced the
275 activation of caspase-1 in monocytes in the same magnitude to the positive control group
276 (Figure 2C and 2D). Moreover, SARS-CoV-2-induced caspase-1 activation was a
277 specific event, since we did not observe activation of the apoptotic caspases-3 and -7 in
278 infected monocytes (Figure 2E and 2F). As caspase-1 activity is critical for the production
279 of IL-1β (19,20), we measured the levels of this cytokine in our experiments. Our data
280 show that SARS-CoV-2 infection was able to increase IL-1β production, this
281 phenomenon being prevented with pretreatment with AC-YVAD-CMK, and not altered
282 with a necroptosis inhibitor. (Figure 2G). Importantly, inhibition of IL-1R engagement
283 reduced SARS-CoV-2-mediated caspase-1 activation and LDH release (Figure S1),
284 suggesting that inflammasome-dependent IL-1β secretion amplify caspase-1 activation
285 and pyroptosis in SARS-CoV-2 infection.

286 **Inflammasome activation amplify pro-inflammatory cytokines secretion in infected**
287 **monocytes**

288 To evaluate the effect of the activation of inflammasome and pyroptosis on the
289 immune response, we quantified the production of key cytokines in the amplification of
290 the inflammatory process observed clinically in a patient during the course of the
291 infection with IL-6 and TNF-α. Remarkably, caspase-1 specific inhibition, but not pan-
292 caspase or RIPK1 inhibitor, also led to lower levels of the pro-inflammatory cytokines
293 IL-6 and TNF-α, highlighting the participation of the caspase-1-IL-1β axis in
294 inflammatory amplification during SARS-CoV-2 infection. (Figure 3A and 3B). To
295 confirm the effects in SARS-CoV-2 infection in the immune response, whether the
296 observed effect is specifically related to inflammasome activation, we evaluated the
297 production of IL-8, in which induction is independent of the inflammasomes pathway.
298 SARS-CoV-2 infection induced a higher IL-8 production, which was not prevented by
299 caspase-1 inhibition (Figure 3C). In addition, inhibition of IL-1R engagement reduced
300 SARS-CoV-2-mediated was able to significantly decrease the production of IL-1 β, IL-
301 6, TNF-α and did not alter the production of IL-8 (Figure S2).

302

303

304 **Infection with SARS-CoV-2 decreases the expression of HLA class II in human**
305 **monocytes independently of the activation of inflammasomes**

306 To investigate the impact of inflammasome activation and cell death through
307 pyroptosis on the orchestration of anti-SARS-CoV-2 immune response, cells were then
308 marked with HLA-DR and analyzed by flow cytometry. We found that SARS-CoV-2
309 infection induced a decrease in HLA-DR expression in monocytes (Figure 4A and 4B).
310 However, the inhibition of caspase-1 (Figure 4A and 4B) and IL-1R engagement (Figure
311 S3) did not prevent the SARS-CoV-2-mediated decreasing of HLA expression. These
312 results suggest that even in disassociation with the engagement of SARS-CoV-2-induced
313 inflammasome activation, monocytes exposed to the new CoV will present limited ability
314 to orchestrate the immune response.

315 **Atazanavir prevented inflammasome-dependent pyroptosis**

316 Given our findings that pyroptosis and decreased HLA-DR expression are
317 triggered during SARS-CoV-2 replication, we tested whether atazanavir (ATV), an HIV
318 protease inhibitor recently shown to possess antiviral activity against the new CoV in
319 monocytes (17), could prevent these events. Flow cytometry analysis of SARS-CoV-2-
320 infected monocytes treated with ATV demonstrated a significant reduction in caspase-1
321 activity, observed by the decreased FAM-YVAD-FLICA labeling (Figure 5A and 5B).
322 Other orally available repurposed anti-SARS-CoV-2 drugs, such as lopinavir (LPV) and
323 ribavirin (RBV), did not affect SARS-CoV-2-induced pyroptosis (Figure 5C). Moreover,
324 treatments with ATV did not alter the activity of caspase-1, -3 and -7 in monocytes
325 exposed to LPS and ATP, used as a positive control of pyroptosis (Figure S4), indicating
326 a specific antiviral activity of this drug. Consistently, treatment with ATV also reduced
327 the levels of IL-1β, IL-6 and TNF-α in SARS-CoV-2-infected monocytes, when
328 compared to the untreated cells (Figure 5D-F). ATV did not interfere with the production
329 of IL-8, which is independent of inflammasome engagement (Figure 5G).

330 We then confirmed whether ATV can prevent SARS-CoV-2-induced pyroptosis.
331 Lower levels of LDH were detected in the supernatants of SARS-CoV-2-infected
332 monocytes treated with ATV, when compared to infected and untreated cells (Figure 5H).
333 The treatment with ATV was also able to prevent the decrease of HLA-DR expression in
334 infected monocytes (Figure 5I and J). LPV and RBV did not alter the HLA-DR expression

335 in monocytes infected with SARS-Cov-2 (Figure S5). Since ATV inhibits the early
336 proteolytic processing of viral antigens, an early event during SARS-CoV-2 replication,
337 this drug represented the most upstream process pharmacologically inhibited in this
338 investigation to prevent pyroptosis and HLA-DR knockdown.

339 **Inflammasome activation and pyroptosis are risk factors in critically ill COVID-19**
340 **patients**

341 To clinically validate our findings, we evaluated if monocytes obtained from
342 critically ill patients with COVID-19 would also display signals of inflammasome
343 engagement and pyroptosis. We observed that monocytes from COVID-19 patients had
344 increased caspase-1 activation (Figure 6A and 6B) and significantly higher PI+ staining,
345 when compared to monocytes from healthy donors (HD) (Figure 6C and 6D).
346 Corroborating with our *in vitro* data, we also detected higher levels of IL-1β in the plasma
347 of critically ill patients (Figure 6E). Therefore, the *in vitro* results from the previous
348 sections stand on the shoulders of the clinical relevance of monocytes in patients with
349 severe COVID-19.

350 **SARS-CoV-2 infection induces inflammasome-dependent pyroptosis and**
351 **downmodulation of HLA-DR monocytes, which can be prevented by atazanavir**

352 A representative scheme to summarize the effect of SARS-CoV-2 infection upon
353 in the increase of TNF-α and IL-6 levels, as part of an immunodysregulation promoted
354 by pyroptosis. SARS-CoV-2-induced pyropotosis engages inflammasomes, to activate
355 caspase-1 and IL-1ß. Release of IL-1ß amplify the activation of inflammasomes during
356 the SARS-CoV-2 infection. In parallel, SARS-CoV-2 also induces the HLA-DR
357 downregulation. ATV prevented SARS-CoV-2-induced deleterious effects on monocyte
358 biology.

359 ## Discussion

360 COVID-19 has caused in less than 8 months over 800,000 deaths worldwide (21)
361 and represent the major public health crisis of the beginning of 21st century, leading to an
362 unpredictable impact in global economics (22,23). SARS-CoV-2 infection triggers an
363 uncontrolled inflammatory response and marked leukopenia with consequent
364 lung/respiratory dysfunction, which are the characteristics of the most severe

365 manifestations of the COVID-19 (24,25). Similarly, to other respiratory viruses (26-29),
366 SARS-CoV-2 induces a cytokine storm, characterized by an uncontrolled inflammatory
367 response mediated by monocytes/macrophages, when they should orchestrate the
368 antiviral immune response (30). In this work, we demonstrate that SARS-CoV-2 infection
369 triggers inflammasome activation, increases IL-1ß secretion by monocytes, resulting in
370 pyroptotic cell death, which could be a key event for SARS-CoV-2 pathogenesis in
371 critically ill patients (31). This deleterious immune dysregulation loop triggered by
372 SARS-CoV-2 may be impaired by ATV.

373 Our results demonstrate that SARS-CoV-2 leads to an intense cell death in human
374 monocytes, observed by the increase in LDH release in infected cultures, as well as by
375 the higher number of PI^+ cells when compared to uninfected controls. Even though the
376 pretreatment of infected monocytes with the pan-caspase inhibitor ZVAD-FMK
377 prevented IL-1β secretion, it was not able to prevent the release of LDH. Indeed, others
378 have demonstrated that the treatment with ZVAD-FMK induces necroptosis in diverse
379 cell types (32-34). Notably, as pyroptosis is an inflammatory and programmed cell death
380 mediated by inflammasome and inflammatory caspase-1 activation (10,11), we
381 investigated the engagement and activation of these structures in human monocytes
382 infected with SARS-CoV-2. Activation of caspase-1 and increased production of IL-1ß
383 were observed in infected monocytes. This is correlated to the activation of
384 inflammasomes, because the pretreatment of infected monocytes with YVAD prevented
385 caspase-1 activation. These *in vitro* results are in accordance with the literature and with
386 our finding described here that indicate the formation of inflammasomes in patients with
387 severe COVID-19 (35). We also showed that the release of IL-1ß could be promoted by
388 the activation of inflammasomes during the SARS-CoV-2 infection, because blockage of
389 IL-1ß receptors reduced caspase-1 activation and cell death. These results corroborate
390 with studies showing that the increase in IL-1ß production is associated with severe
391 COVID-19 (36-38). Under our experimental conditions, the increase in IL-1ß precedes
392 the unbalanced IL-6 release. These information should not be neglected when considering
393 biopharmaceuticals to tackle cytokine storm in severe COVID-19.

394 Monocytes that survived from SARS-CoV-2 infection displayed decreased HLA-
395 DR expression, which has also been described in monocytes isolated from COVID-19
396 patients (39,40). Our results suggest that this modulation of HLA expression is not

397 directly associated with the activation of inflammasomes, and may be involved by other
398 inflammatory pathways, since we and others have observed increased levels of IL-6 by
399 myeloid cells impairing HLA-DR membrane expression (41).

400 To stablish the clinical relevance of SARS-CoV-2-induced pyroptosis in
401 monocytes (41,41), we analyzed peripheral monocytes isolated from patients with severe
402 COVID-19. We found that the cells from the patients displayed higher caspase-1
403 activation, when compared with monocytes isolated from HD. Recent clinical data reveal
404 high levels of LDH and consistent leukopenia in critically ill COVID-19 patients
405 (6,7,35,42-44). Our data also demonstrate intense monocyte death in COVID-19 patients,
406 as detected through flow cytometry analyzes. Altogether, these data suggest that the
407 severity of COVID-19 may be associated with inflammasome activation in monocytes
408 that results in large amounts of IL-1ß and generates an excessive inflammatory response,
409 further characterized by high levels of IL-6 and TNF-α. Consistently, treatment with IL-
410 1RA has been associated with clinical and inflammatory improvements in critically ill
411 COVID-19 patients (45). These results are in line with clinical case reports that
412 demonstrate that monocytes/macrophages are key cells in the deleterious pro-
413 inflammatory events that characterize the most serious cases of COVID-19 (46-49).

414 To the best of our knowledge, effective therapies for COVID-19 should ideally
415 combine antiviral/anti-inflammatory drugs to reduce viral load and to mitigate the
416 cytokine storm. In the present study, we showed that ATV, an antiretroviral approved in
417 2003 for HIV-1 treatment and previously described by us as having anti-SARS-CoV-2
418 effects in different cell types (including monocytes)(50), to block new CoV-induced
419 pyroptosis and HLA-DR knockdown in monocytes. In addition, ATV inhibited the
420 release of LDH and the production of IL-1ß, f IL-6 and TNF-α from SARS-CoV-2-
421 infected monocytes, which are key players in the cytokine storm associated with COVID-
422 19 (51,52).

423 In this work, we originally describe that infection with SARS-CoV-2 can induce
424 pyroptotic cell death by inflammasome activation, which may be related to the intense
425 leukopenia and exacerbated inflammation seen in severe cases of the COVID-19. Since
426 there is no specific therapy for this disease, our results point out that ATV has a promising
427 therapeutic potential against SARS-CoV-2-induced cell death.

Acknowledgments and funding

We thank the Hemotherapy Service from Hospital Clementino Fraga Filho (Federal University of Rio de Janeiro, Brazil) for providing buffy-coats. This work was supported by grants from Fundação de Amparo a Pesquisa do Estado do Rio de Janeiro (FAPERJ), Inova Fiocruz, Conselho Nacional de Desenvolvimento Científico e Tecnológico (CNPq) and Coordenação de Aperfeiçoamento de Pessoal de Nível Superior (CAPES) and Mercosur Fund for Structural Convergence (FOCEM, Mercosur, grant number 03/11) granted for Thiago Moreno L. Souza, Patrícia T. Bozza, Fernando A. Bozza and Dumith Chequer Bou-Habib. Funding was also provided by CNPq, CAPES and FAPERJ through the National Institutes of Science and Technology Program (INCT) to Carlos Morel (INCT-IDPN) and to Wilson Savino (INCT-NIM). Thanks are due to Oswaldo Cruz Foundation/Fiocruz under the auspicious of Inova program. The funding sponsors had no role in the design of the study; in the collection, analyses, or interpretation of data; in the writing of the manuscript, and in the decision to publish the results.

References

1. Conti P, Ronconi G, Caraffa A, Gallenga CE, Ross R, Frydas I, et al. Induction of pro-inflammatory cytokines (IL-1 and IL-6) and lung inflammation by COVID-19: anti-inflammatory strategies. Journal of biological regulators and homeostatic agents. 2020.
2. Long B, Brady WJ, Koyfman A, Gottlieb M. Cardiovascular complications in COVID-19. American Journal of Emergency Medicine. 2020.
3. Li J, Fan J-G. Characteristics and Mechanism of Liver Injury in 2019 Coronavirus Disease. J Clin Transl Hepatol. 2020.
4. Giamarellos-Bourboulis EJ, Netea MG, Rovina N, Akinosoglou K, Antoniadou A, Antonakos N, et al. Cell Host Microbe. 2020.
5. Du RH, Liang LR, Yang CQ, Wang W, Cao TZ, Li M, et al. Predictors of mortality for patients with COVID-19 pneumonia caused by SARSCoV- 2: A prospective cohort study. Eur Respir J. 2020.

457 6. Zhou F, Yu T, Du R, Fan G, Liu Y, Liu Z, et al. Clinical course and risk factors
458 for mortality of adult inpatients with COVID-19 in Wuhan, China: a
459 retrospective cohort study. Lancet. 2020.
460 7. Wölfel R, Corman VM, Guggemos W, Seilmaier M, Zange S, Müller MA, et
461 al. Virological assessment of hospitalized patients with COVID-2019. Nature.
462 2020.
463 8. Wang J, Jiang M, Chen X, Montaner LJ. Cytokine storm and leukocyte
464 changes in mild versus severe SARS-CoV-2 infection: Review of 3939
465 COVID-19 patients in China and emerging pathogenesis and therapy
466 concepts. Journal of Leukocyte Biology. 2020.
467 9. Chen Z, John Wherry E. T cell responses in patients with COVID-19. Nature
468 Reviews Immunology. 2020.
469 10. Danthi P. Viruses and the Diversity of Cell Death. Annual Review of
470 Virology. 2016.
471 11. Jorgensen I, Miao EA. Pyroptotic cell death defends against intracellular
472 pathogens. Immunological Reviews. 2015.
473 12. Man SM, Karki R, Kanneganti TD. Molecular mechanisms and functions of
474 pyroptosis, inflammatory caspases and inflammasomes in infectious diseases.
475 Immunological Reviews. 2017.
476 13. Xu Z, Shi L, Wang Y, Zhang J, Huang L, Zhang C, et al. Pathological findings
477 of COVID-19 associated with acute respiratory distress syndrome. Lancet
478 Respir Med. 2020.
479 14. Han Y, Zhang H, Mu S, Wei W, Jin C, Xue Y, et al. Lactate dehydrogenase,
480 a Risk Factor of Severe COVID-19 Patients. medRxiv. 2020.
481 15. Terpos E, Ntanasis-Stathopoulos I, Elalamy I, Kastritis E, Sergentanis TN,
482 Politou M, et al. Hematological findings and complications of COVID-19.
483 American Journal of Hematology. 2020.
484 16. Li YX, Wu W, Yang T, Zhou W, Fu YM, Feng QM, et al. [Characteristics of
485 peripheral blood leukocyte differential counts in patients with COVID-19].
486 Zhonghua nei ke za zhi. 2020.
487 17. Ding X, Yu Y, Lu B, Huo J, Chen M, Kang Y, et al. Dynamic profile and
488 clinical implications of hematological parameters in hospitalized patients with
489 coronavirus disease 2019. Clin Chem Lab Med. 2020.

490 18. Singh A, Sood N, Narang V, Goyal A. Morphology of COVID-19-affected
491 cells in peripheral blood film. BMJ Case Reports. 2020.
492 19. Zalinger ZB, Elliott R, Weiss SR. Role of the inflammasome-related cytokines
493 Il-1 and Il-18 during infection with murine coronavirus. J Neurovirol. 2017.
494 20. Franchi L, Eigenbrod T, Muñoz-Planillo R, Nuñez G. The inflammasome: A
495 caspase-1-activation platform that regulates immune responses and disease
496 pathogenesis. Nature Immunology. 2009.
497 21. OPAS. COVID-19 (doença causada pelo novo coronavírus). Folha Inf. 2020.
498 22. Dong E, Du H, Gardner L. An interactive web-based dashboard to track
499 COVID-19 in real time. The Lancet Infectious Diseases. 2020.
500 23. Wissel BD, Van Camp PJ, Kouril M, Weis C, Glauser TA, White PS, et al. An
501 Interactive Online Dashboard for Tracking COVID-19 in U.S. Counties,
502 Cities, and States in Real Time. J Am Med Inform Assoc. 2020.
503 24. Lucas C, Wong P, Klein J, Castro TBR, Silva J, Sundaram M, et al.
504 Longitudinal analyses reveal immunological misfiring in severe COVID-19.
505 Nature. 2020.
506 25. Tay MZ, Poh CM, Rénia L, MacAry PA, Ng LFP. The trinity of COVID-19:
507 immunity, inflammation and intervention. Nature Reviews Immunology.
508 2020.
509 26. Teijaro JR. The role of cytokine responses during influenza virus pathogenesis
510 and potential therapeutic options. Curr Top Microbiol Immunol. 2014.
511 27. Szretter KJ, Gangappa S, Lu X, Smith C, Shieh W-J, Zaki SR, et al. Role of
512 Host Cytokine Responses in the Pathogenesis of Avian H5N1 Influenza
513 Viruses in Mice. J Virol. 2007.
514 28. Peschke T, Bender A, Nain M, Gemsa D. Role of Macrophage Cytokines in
515 Influenza A Virus lnfections. Immunobiology. 1993.
516 29. Woo PCY, Tung ETK, Chan KH, Lau CCY, Lau SKP, Yuen KY. Cytokine
517 profiles induced by the novel swine-origin influenza A/H1N1 virus:
518 Implications for treatment strategies. J Infect Dis. 2010.
519 30. Jamilloux Y, Henry T, Belot A, Viel S, Fauter M, El Jammal T, et al. Should
520 we stimulate or suppress immune responses in COVID-19? Cytokine and anti-
521 cytokine interventions. Autoimmunity Reviews. 2020.

522 31. Zheng Z, Peng F, Xu B, Zhao J, Liu H, Peng J, et al. Risk factors of critical &
523 mortal COVID-19 cases: A systematic literature review and meta-analysis.
524 Journal of Infection. 2020.
525 32. Siegmund D, Kums J, Ehrenschwender M, Wajant H. Activation of TNFR2
526 sensitizes macrophages for TNFR1-mediated necroptosis. Cell Death Dis.
527 2016.
528 33. Kim SJ, Li J. Caspase blockade induces RIP3-mediated programmed necrosis
529 in Toll-like receptor-activated microglia. Cell Death Dis. 2013.
530 34. Wu YT, Tan HL, Huang Q, Sun XJ, Zhu X, Shen HM. ZVAD-induced
531 necroptosis in L929 cells depends on autocrine production of TNFα mediated
532 by the PKC-MAPKs-AP-1 pathway. Cell Death Differ. 2011.
533 35. Rodrigues S, de Sá KS, Ishimoto AY, Becerra A, Oliveira S, Almeida L, et al.
534 Inflammasome activation in COVID-19 patients 1 2 Tamara. medRxiv. 2020;
535 36. Abbasifard M, Khorramdelazad H. The bio-mission of interleukin-6 in the
536 pathogenesis of COVID-19: A brief look at potential therapeutic tactics. Life
537 Sciences. 2020.
538 37. Yao Z, Zheng Z, Wu K, Zheng J. Immune environment modulation in
539 pneumonia patients caused by coronavirus: SARS-CoV, MERS-CoV and
540 SARS-CoV-2. Aging (Albany NY). 2020.
541 38. Zhang Y, Li J, Zhan Y, Wu L, Yu X, Zhang W, et al. Analysis of serum
542 cytokines in patients with severe acute respiratory syndrome. Infect Immun.
543 2004.
544 39. Ong EZ, Chan YFZ, Leong WY, Lee NMY, Kalimuddin S, Haja Mohideen
545 SM, et al. A Dynamic Immune Response Shapes COVID-19 Progression. Cell
546 Host Microbe. 2020.
547 40. Laing AG, Lorenc A, del Molino del Barrio I, Das A, Fish M, Monin L, et al.
548 A dynamic COVID-19 immune signature includes associations with poor
549 prognosis. Nat Med [Internet]. 2020; Available from:
550 https://doi.org/10.1038/s41591-020-1038-6.
551 41. Ohno Y, Kitamura H, Takahashi N, Ohtake J, Kaneumi S, Sumida K, et al. IL-
552 6 down-regulates HLA class II expression and IL-12 production of human
553 dendritic cells to impair activation of antigen-specific CD4+ T cells. Cancer
554 Immunol Immunother. 2016.

42. Yap JKY, Moriyama M, Iwasaki A. Inflammasomes and Pyroptosis as Therapeutic Targets for COVID-19. J Immunol. 2020.
43. Yuan J, Zou R, Zeng L, Kou S, Lan J, Li X, et al. The correlation between viral clearance and biochemical outcomes of 94 COVID-19 infected discharged patients. Inflamm Res. 2020.
44. Yan L, Zhang HT, Goncalves J, Xiao Y, Wang M, Guo Y, et al. An interpretable mortality prediction model for COVID-19 patients. Nat Mach Intell. 2020.
45. Cauchois R, Koubi M, Delarbre D, Manet C, Carvelli J, Blasco VB, et al. Early IL-1 receptor blockade in severe inflammatory respiratory failure complicating COVID-19. Proc Natl Acad Sci. 2020.
46. Qin C, Zhou L, Hu Z, Zhang S, Yang S, Tao Y, et al. Dysregulation of immune response in patients with COVID-19 in Wuhan, China. Clin Infect Dis. 2020.
47. McGonagle D, Sharif K, O'Regan A, Bridgewood C. The Role of Cytokines including Interleukin-6 in COVID-19 induced Pneumonia and Macrophage Activation Syndrome-Like Disease. Autoimmunity Reviews. 2020.
48. Merad M, Martin JC. Pathological inflammation in patients with COVID-19: a key role for monocytes and macrophages. Nature Reviews Immunology. 2020.
49. Park MD. Macrophages: a Trojan horse in COVID-19? Nat Rev Immunol. 2020.
50. Fintelman-Rodrigues N, Sacramento CQ, Lima CR, Silva FS da, Ferreira A, Mattos M, et al. Atazanavir inhibits SARS-CoV-2 replication and pro-inflammatory cytokine production. bioRxiv. 2020.
51. Hantoushzadeh S, Norooznezhad AH. Possible Cause of Inflammatory Storm and Septic Shock in Patients Diagnosed with (COVID-19). Arch Med Res. 2020.
52. Hantoushzadeh S, Norooznezhad AH. Inappropriate Antibiotic Consumption as a Possible Cause of Inflammatory Storm and Septic Shock in Patients Diagnosed with Coronavirus Disease 2019 (COVID-19). Arch Med Res. 2020.

590 **FIGURE LEGENDS**
591
592 **Figure 1. SARS-Cov-2 induces monocyte cell death through pyroptosis.** Human
593 monocytes were infected with SARS-CoV-2 (MOI 0.1) for 24 h. As a positive control,
594 monocytes were stimulated with LPS (500ng/mL) for 23 h and after this time, incubated
595 with ATP (2 mM) for 1 h. **(A)** Cell viability was assessed through the measurement of
596 LDH release in the supernatant of monocytes. **(B, C and D)** Monocytes` monolayers were
597 stained with propidium iodide (PI) plus Annexin V and pyroptotic cell death were
598 determine by flow cytometer analysis and **(E)** labeled with DAPI to visualize the nuclei
599 fluorescence microscopy. Images and Graph data are representative of six independent
600 experiments. Data are presented as the mean ± SEM * $P < 0.05$ *versus* control group
601 (MOCK).

602 **Figure 2. SARS-CoV-2 induce inflammasome activation in human monocytes.**
603 Human monocytes were pretreated with caspase-1 inhibitor (AC-YVAD-CMK – 1 μM),
604 pan-caspase inhibitor (ZVAD-FMK - 10 μM) or necroptosis inhibitor (Nec-1 - 25 μM)
605 for 1 h and infected with SARS-Cov-2 (MOI 0.1) for 24 h. Monocytes were stimulated
606 with LPS (500ng/mL) for 23 h and after this time were stimulated with ATP (2 mM) for
607 1 h as a positive control group for the formation of inflammasomes and pyroptosis
608 induction. **(A, B)** Monocytes` monolayers were used for determination of the levels of
609 pro-caspase-1 and cleaved caspase-1 by western blot analysis. **(C - F)** Monocytes were
610 stained with FAM-YVAD-FLICA and FAM-FLICA to determine the caspase-1 and
611 caspase-3/7 activity, respectively, by flow cytometry. **(G)** Cell culture supernatants were
612 collected for the measurement of the levels of IL-1β. Western blot, histogram and graph
613 data are representative of six independent experiments. Data are presented as the mean ±
614 SEM $^{\#}$ $P < 0.05$ *versus* infected and untreated group.

615 **Figure 3. Inflammasome activation amplify pro-inflammatory cytokines secretion**
616 **in infected monocytes.** Human monocytes were pretreated with caspase-1 inhibitor (AC-
617 YVAD-CMK – 1 μM), pan-caspase inhibitor (ZVAD-FMK - 10 μM), necroptosis
618 inhibitor (Nec-1 - 25 μM) or with inhibitor of IL-1ß receptor (IL-1RA – 1 μM).
619 Monocytes were stimulated with LPS (500ng/mL) for 23 h and after this time were
620 stimulated with ATP (2 mM) for 1 h as a positive control group for the formation of
621 inflammasomes and pyroptosis induction. Cell culture supernatants were collected for the
622 measurement of the levels of **(A)** IL-6, **(B)** TNF-α and **(C)** IL-8. Graphs data are

representative of six independent experiments. Data are presented as the mean ± SEM [#] $P < 0.05$ *versus* infected and untreated group.

Figure 4. Infection with SARS-CoV-2 decreases the expression of HLA in human monocytes independently of the activation of inflammasomes. Human monocytes were pretreated with caspase-1 inhibitor (AC-YVAD-CMK – 1 μM) for 1 h and infected with SARS-Cov-2 for 24 h. **(A, B)** Monocytes were stained with HLA-DR APC.H7 or Isotype control APC.H7 to determine the HLA-DR expression by flow cytometry. Mean fluorescence intensity (MFI) value for each sample was represented in graphics. Histogram and graphs datas are representative of six independent experiments. Data are presented as the mean ± SEM [*] $P < 0.05$ *versus* uninfected group (MOCK).

Figure 5. Atazanavir prevented inflammasome-dependent pyroptosis. Human monocytes were infected with SARS-Cov-2 and treated with atazanavir – ATV (10 μM), ribavirina (10 μM) or Lopinavir (10 μM) for 24 h. **(A, B and C)** Monocytes were stained with FAM-YVAD-FLICA or FAM-FLICA and HLA-DR APC.H7 or IgG APC.H7 to determine the caspase-1 and caspase-3/7 activity and HLA-DR expression, respectively and analyzed by flow cytometry. **(D – G)** Culture supernatants were collected and the levels of IL-1β, IL-6, TNF-α and IL-8 were determined by ELISA. **(H)** Assessment of cell viability through the measurement of LDH release in the supernatant of monocytes. **(I and J)** Monocytes were stained with HLA-DR APC.H7 to determine the HLA-DR expression by flow cytometry. Histogram and graphs datas are representative of six independent experiments. Data are presented as the mean ± SEM [*] $P < 0.05$ *versus* control group (MOCK); [#] $P < 0.05$ *versus* only infected group.

Figure 6. Inflammasome activation and pyroptosis are risk factors in critically ill COVID-19 patients. Monocytes isolated from blood samples of critically ill patients with COVID-19 and healthy donors. **(A and B)** monocytes were stained with FAM-YVAD-FLICA or **(C and D)** propidium iodide (PI) and analyzed by flow cytometry. **(E)** plasma was separated and the levels of IL-1β were determined by ELISA. Western blot, histogram and graphs datas are representative of 9 critically ill patients and 8 healthy donors. Data are presented as the mean ± SEM [*] $P < 0.05$ *versus* healthy donors (HD).

Figure 7. Representative scheme of the SARS-CoV-2 infection in activation of inflammasome and pyroptosis in monocyte with downregulation of HLA-DR expression and effects of ATV treatment in this phenomenon.

Table 1: Characteristics of COVID-19 patients and control subjects.

Characteristics[1]	Control (N=8)	Covid-19 (N=9)
Age, years	52.6 (47 – 60)	61 (33 – 79)
Sex, male	8 (100 %)	6 (66.7 %)
Respiratory support		
Oxygen supplementation	0 (0 %)	3 (33.3 %)
Mechanical ventilation	0 (0 %)	6 (66.7 %)
SAPS 3		59.25 (31 – 75)
PaO2/FiO2 ratio	-	210.75 (87 – 509.5)
Vasopressor	-	3 (33.3 %)
Time from symptom onset to blood sample, days	-	10 (6 – 18)
Status on Jun 30th		
Dead	-	5 (55.55 %)
Discharged	-	1 (11.1 %)
Hospitalized	-	3 (33.3 %)
Comorbidities		
Obesity	1 (11.1 %)	1 (11.1 %)
Hypertension	3 (33.3%)	3 (33.3 %)
Diabetes	0 (0%)	0 (0 %)
Cancer	0 (0%)	0 (0 %)
Chronic heart disease[2]	0 (0%)	0 (0 %)
Presenting symptoms		
Cough	0 (0 %)	3 (33,3 %)
Fever	0 (0 %)	3 (33,3 %)
Dyspnea	0 (0 %)	4 (44,4 %)
Headache	0 (0 %)	0 (0 %)
Anosmia	0 (0 %)	0 (0 %)
Laboratory findings on admission		
Lymphocyte count, cells/mm^3	-	1,355.8 (552 –2,564)
Platelet count, x 1000/mm^3	-	169.6 (92 – 278)
Leukocytes	-	8,036 (8.03-18,670)
C Reactive Protein, mg/L	-	14.78 (0.1 – 30.8)

FIGURE 1

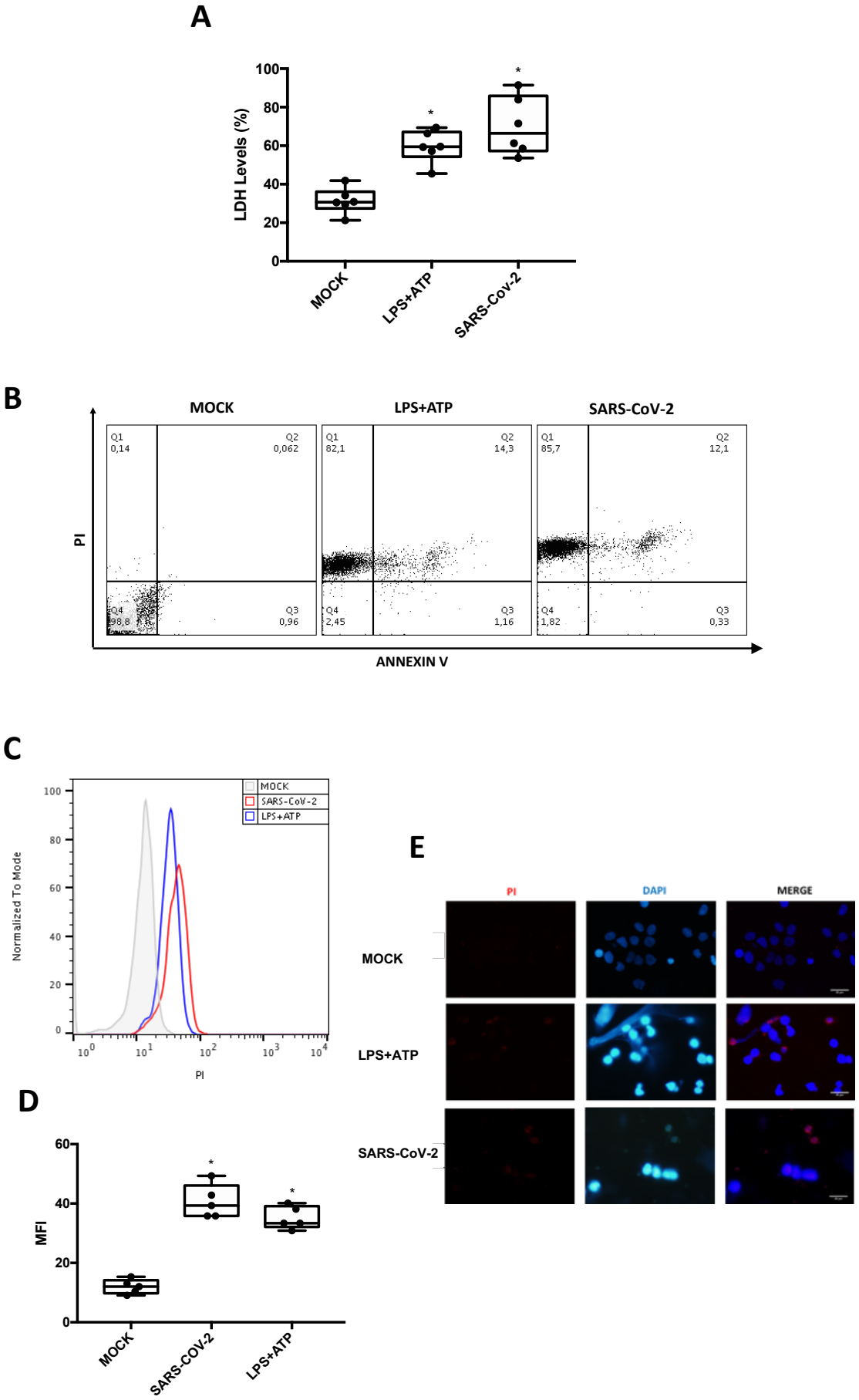
A
LDH Levels (%)
100
80
60
40
20
0
MOCK
LPS+ATP
SARS-CoV-2
B
MOCK
LPS+ATP
SARS-CoV-2
Q1 0,14
Q2 0,062
Q4 98,8
Q3 0,96
Q1 82,1
Q2 14,3
Q4 2,45
Q3 1,16
Q1 85,7
Q2 12,1
Q4 1,82
Q3 0,33
PI
ANNEXIN V
C
MOCK
SARS-CoV-2
LPS+ATP
Normalized To Mode
PI
D
MFI
MOCK
SARS-COV-2
LPS+ATP
E
PI
DAPI
MERGE
MOCK
LPS+ATP
SARS-CoV-2

FIGURE 2

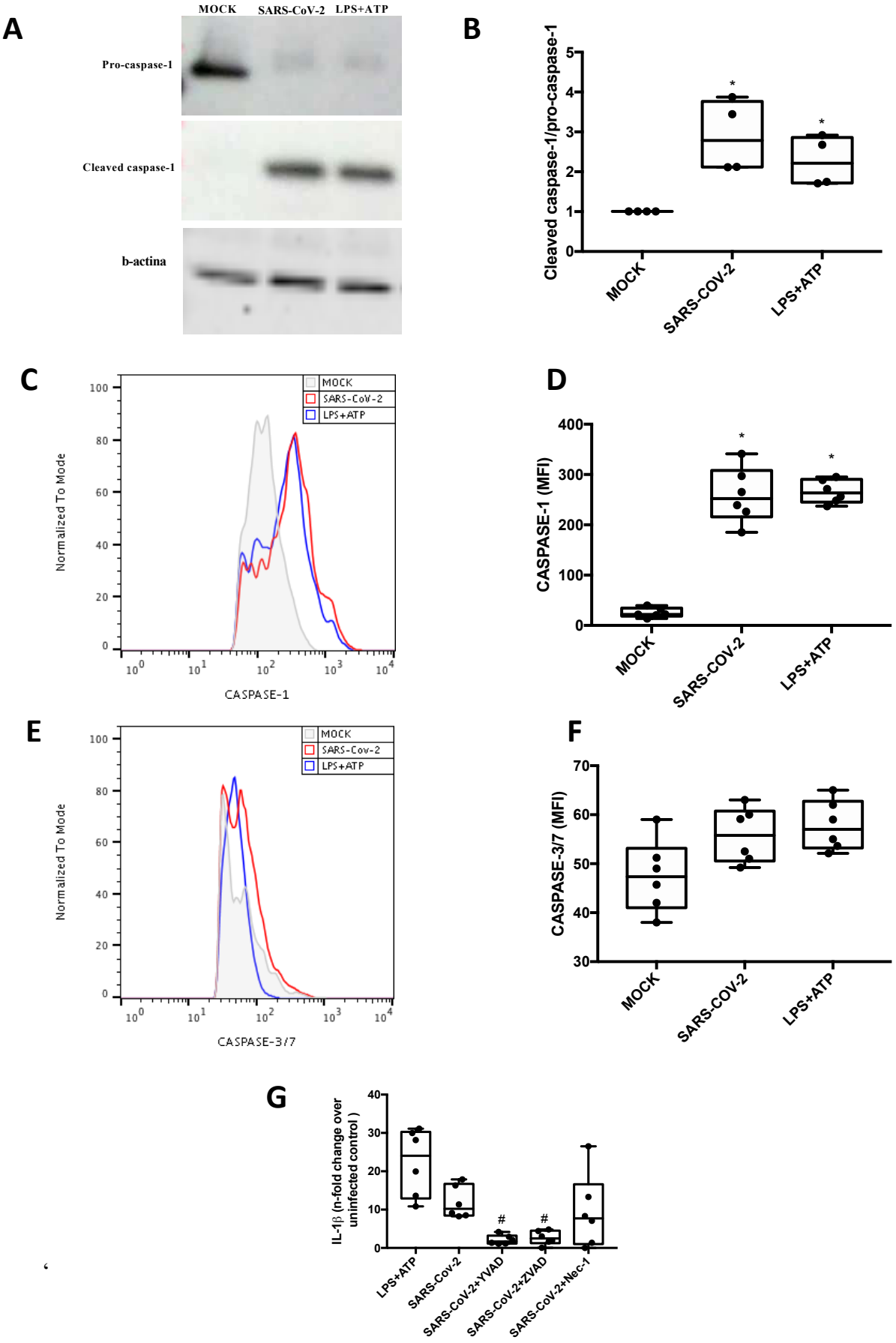
A
MOCK
SARS-CoV-2
LPS+ATP
Pro-caspase-1
Cleaved caspase-1
b-actina
B
Cleaved caspase-1/pro-caspase-1
MOCK
SARS-COV-2
LPS+ATP
C
MOCK
SARS-CoV-2
LPS+ATP
Normalized To Mode
CASPASE-1
D
CASPASE-1 (MFI)
MOCK
SARS-COV-2
LPS+ATP
E
MOCK
SARS-Cov-2
LPS+ATP
Normalized To Mode
CASPASE-3/7
F
CASPASE-3/7 (MFI)
MOCK
SARS-COV-2
LPS+ATP
G
IL-1β (n-fold change over uninfected control)
LPS+ATP
SARS-Cov-2
SARS-CoV-2+YVAD
SARS-CoV-2+ZVAD
SARS-CoV-2+Nec-1

FIGURE 3

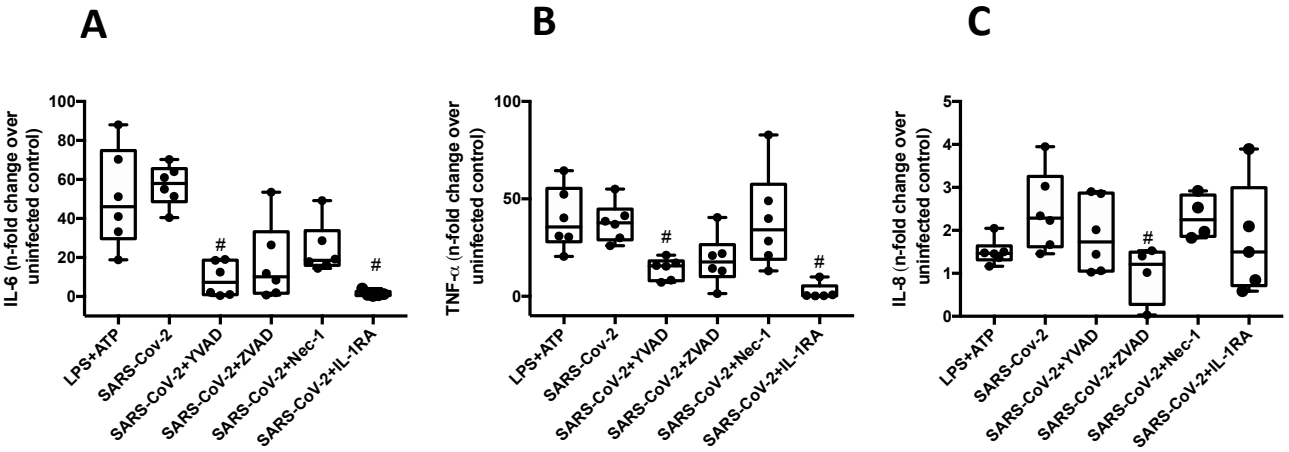
A
B
C
IL-6 (n-fold change over uninfected control)
TNF-α (n-fold change over uninfected control)
IL-8 (n-fold change over uninfected control)
LPS+ATP
SARS-Cov-2
SARS-CoV-2+YVAD
SARS-CoV-2+ZVAD
SARS-CoV-2+Nec-1
SARS-CoV-2+IL-1RA
#

FIGURE 4

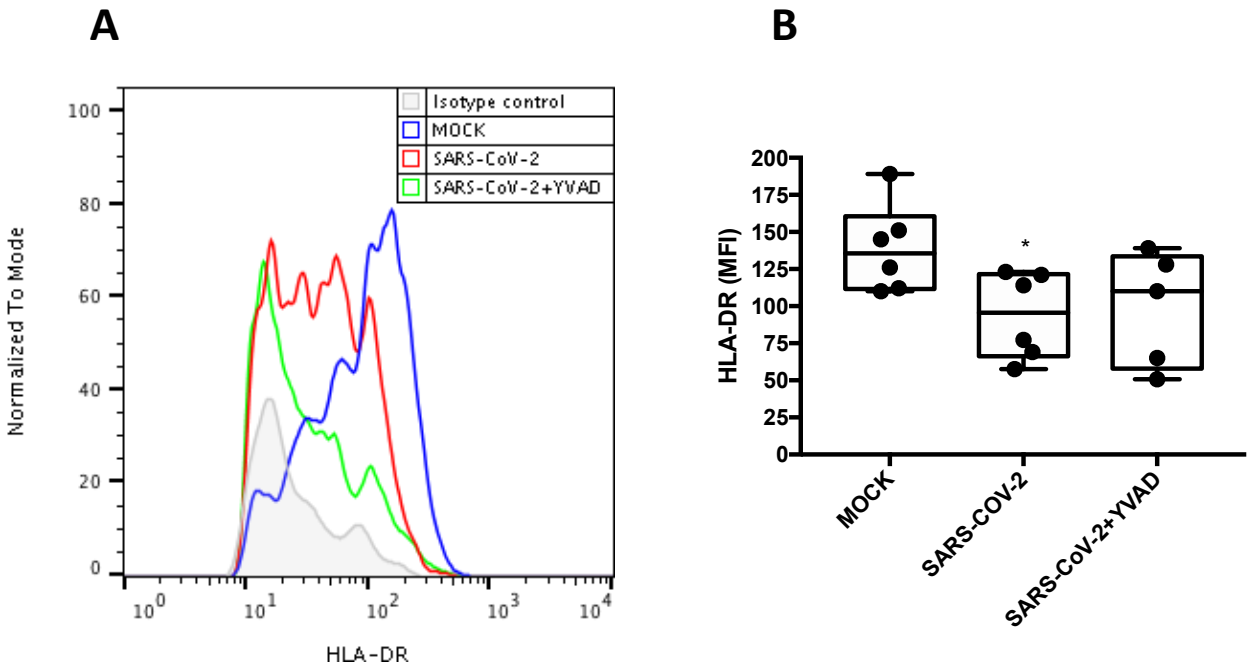
A
Isotype control
MOCK
SARS-CoV-2
SARS-CoV-2+YVAD
Normalized To Mode
HLA-DR
B
HLA-DR (MFI)
MOCK
SARS-COV-2
SARS-CoV-2+YVAD

FIGURE 5

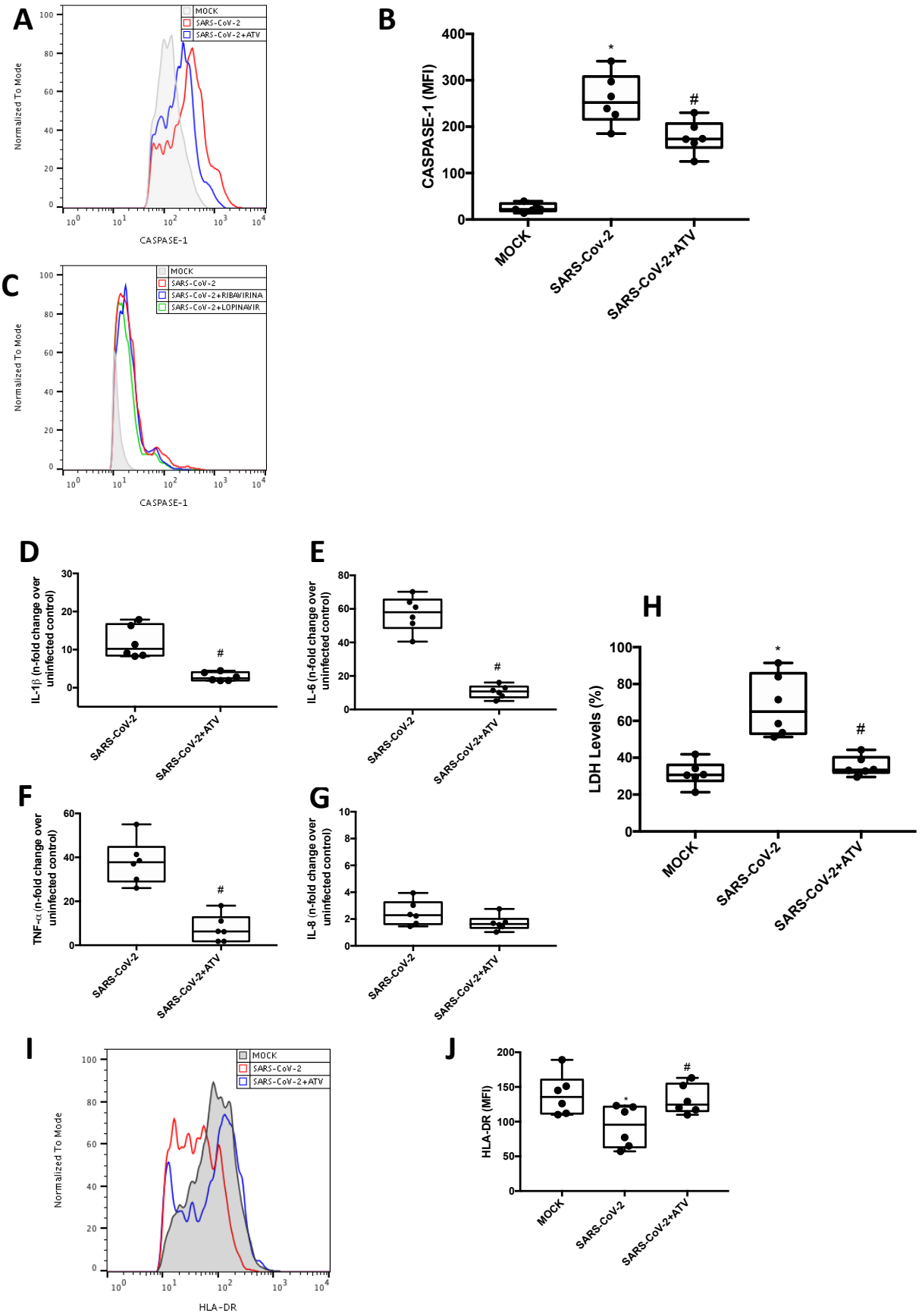
A
MOCK
SARS-CoV-2
SARS-CoV-2+ATV
Normalized To Mode
CASPASE-1
B
CASPASE-1 (MFI)
MOCK
SARS-Cov-2
SARS-CoV-2+ATV
C
MOCK
SARS-CoV-2
SARS-CoV-2+RIBAVIRINA
SARS-CoV-2+LOPINAVIR
Normalized To Mode
CASPASE-1
D
IL-1β (n-fold change over uninfected control)
SARS-CoV-2
SARS-CoV-2+ATV
E
IL-6 (n-fold change over uninfected control)
SARS-CoV-2
SARS-CoV-2+ATV
H
LDH Levels (%)
MOCK
SARS-CoV-2
SARS-CoV-2+ATV
F
TNF-α (n-fold change over uninfected control)
SARS-CoV-2
SARS-CoV-2+ATV
G
IL-8 (n-fold change over uninfected control)
SARS-CoV-2
SARS-CoV-2+ATV
I
MOCK
SARS-CoV-2
SARS-CoV-2+ATV
Normalized To Mode
HLA-DR
J
HLA-DR (MFI)
MOCK
SARS-CoV-2
SARS-CoV-2+ATV

FIGURE 6

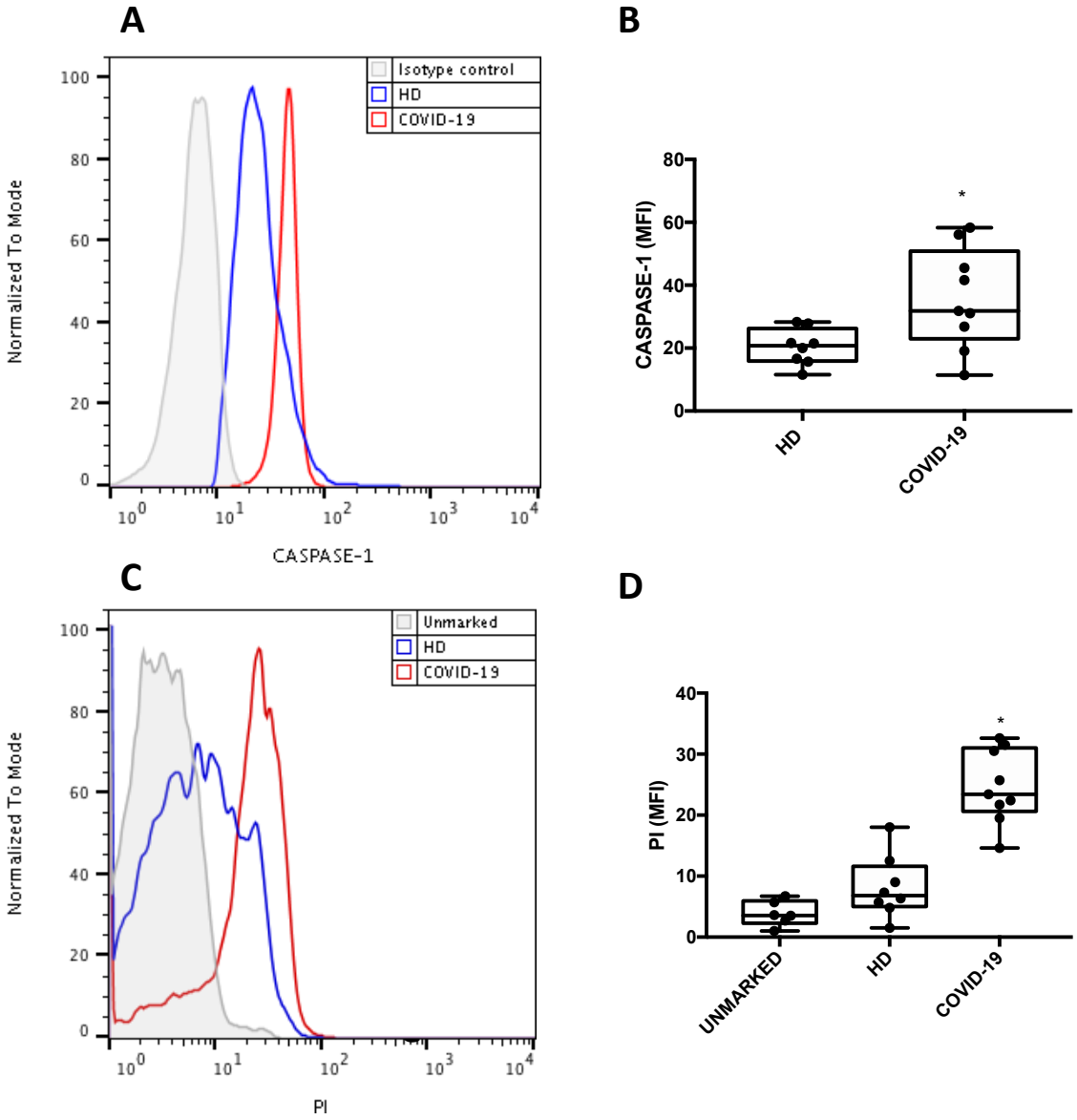
A
Isotype control
HD
COVID-19
Normalized To Mode
CASPASE-1
B
CASPASE-1 (MFI)
HD
COVID-19
C
Unmarked
HD
COVID-19
Normalized To Mode
PI
D
PI (MFI)
UNMARKED
HD
COVID-19

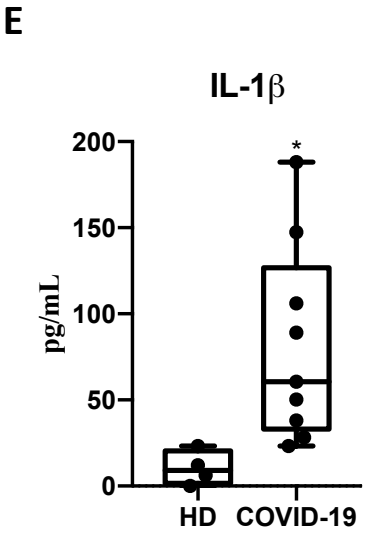
E
IL-1β
pg/mL
HD
COVID-19

FIGURE 7

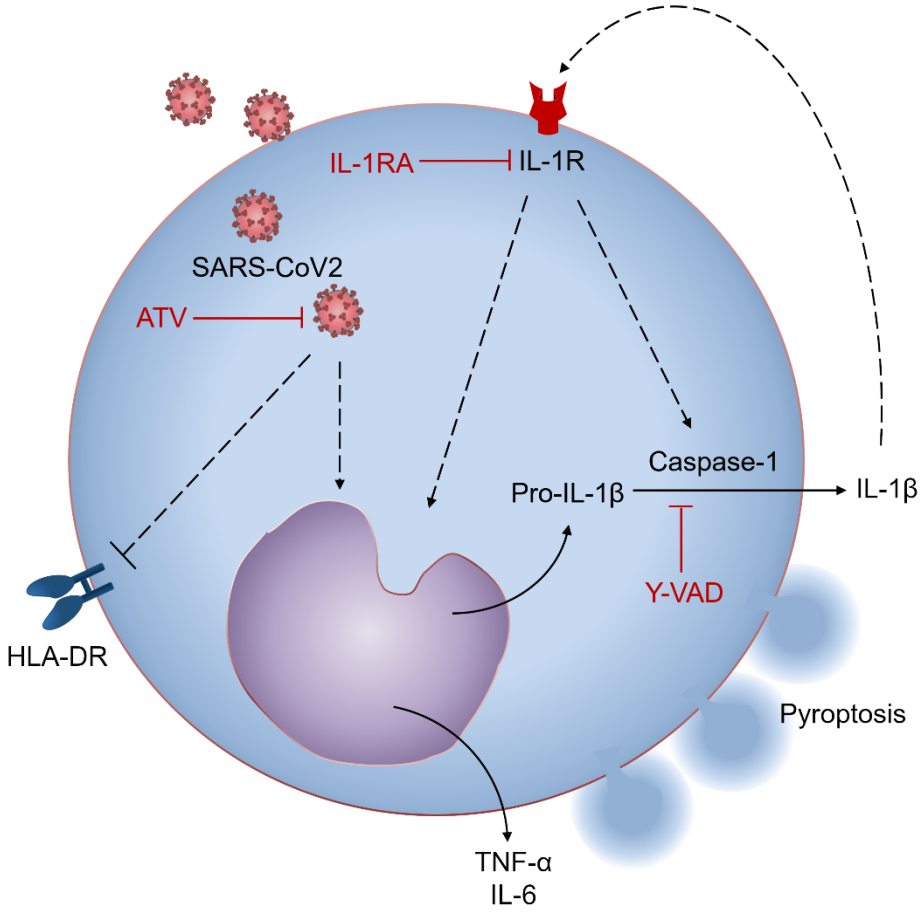
IL-1RA
IL-1R
SARS-CoV2
ATV
Caspase-1
Pro-IL-1β
IL-1β
Y-VAD
HLA-DR
Pyroptosis
TNF-α
IL-6

FIGURE S1

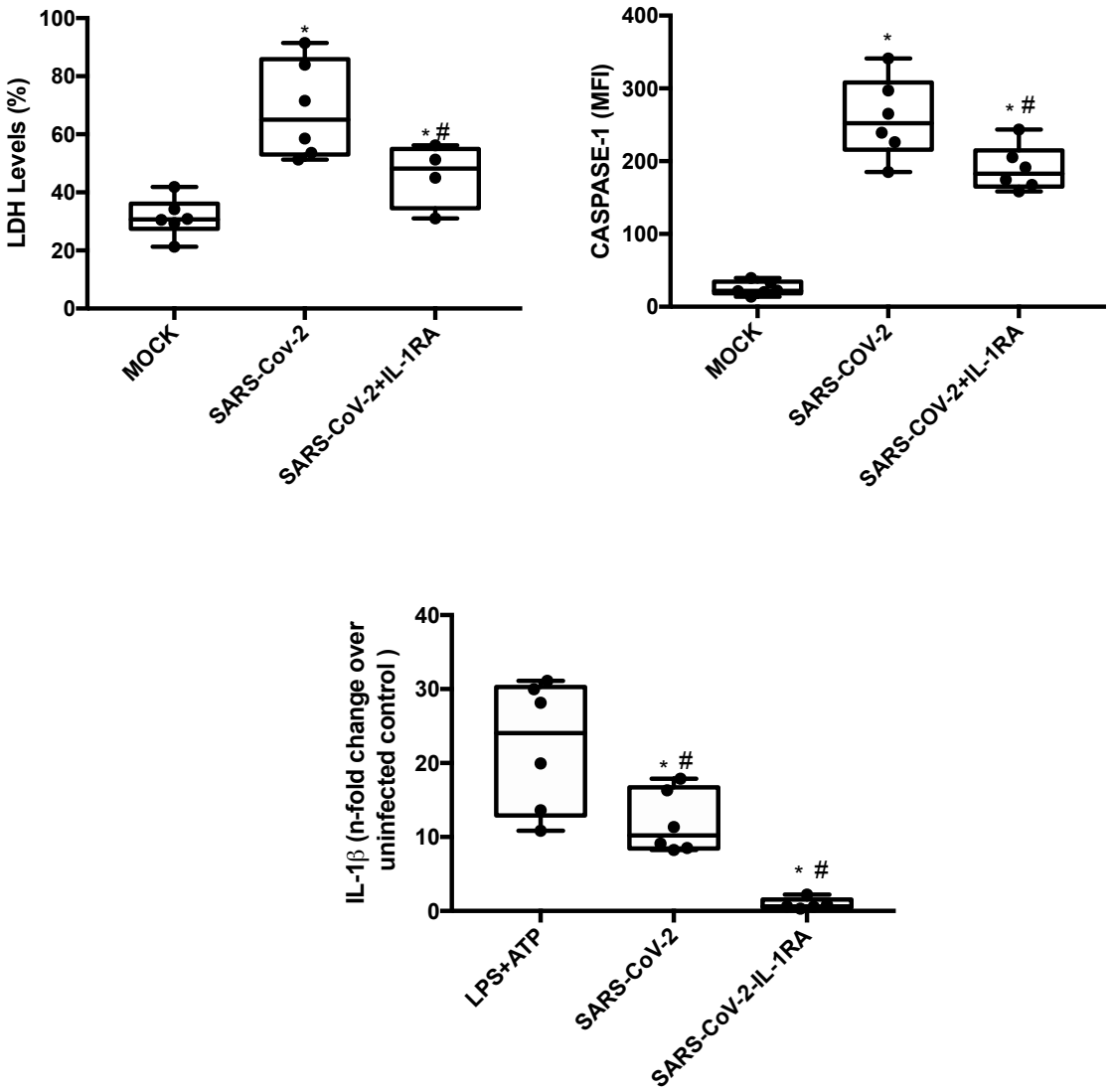

S1 Fig. SARS-CoV-2 induce inflammasome activation and pyroptosis in human monocytes by IL-1β amplification. Human monocytes were pretreated with IL-1β receptor (IL-1RA – 1 μM) for 1 h and infected with SARS-Cov-2 (MOI 0.1) for 24 h. Cell viability was assessed through the measurement of LDH release in the supernatant and monocytes were stained with FAM-YVAD-FLICA to determine the caspase-1 and caspase-3/7 activity, respectively, by flow cytometry. Cell culture supernatants also were collected for the measurement of the levels of IL-1β. Data are presented as the mean ± SEM $^{\#}$ $P < 0.05$ *versus* infected and untreated group; * $P < 0.05$ *versus* control group (MOCK). Graphs are representative of four independent experiments.

997 **FIGURE S2**

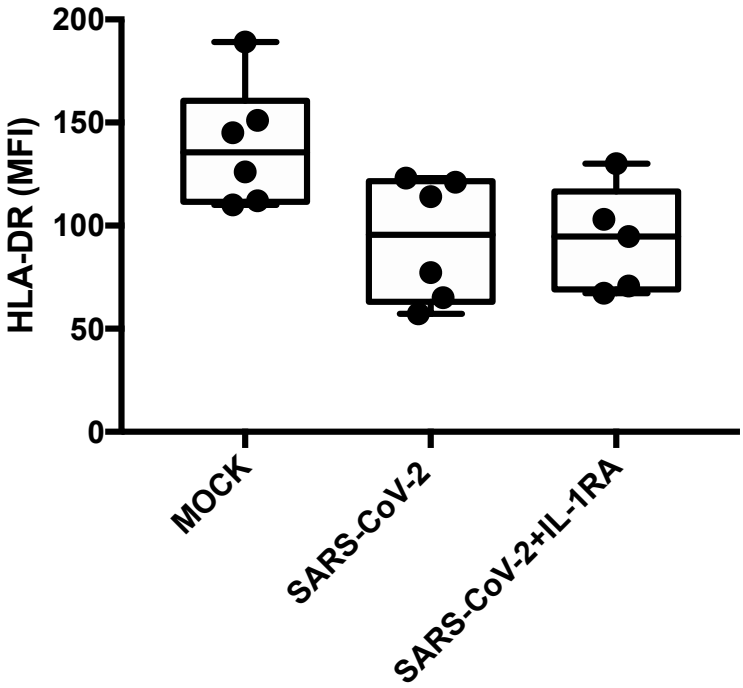

1024 **S2 Fig. Infection with SARS-CoV-2 decreases the expression of HLA in human**
1025 **monocytes independently of the IL-1ß activation.** Human monocytes were pretreated
1026 with inhibitor of IL-1ß receptor (IL-1RA – 1 μM) for 1 h and infected with SARS-Cov-
1027 2 for 24 h. Monocytes were stained with HLA-DR APC.H7 or IgG APC.H7 to determine
1028 the HLA-DR expression by flow cytometry. Mean fluorescence intensity (MFI) value for
1029 each sample was represented in graphics. Graphs datas are representative of four
1030 independent experiments. Data are presented as the mean ± SEM $^{\#}$ $P < 0.05$ *versus*
1031 uninfected group (MOCK).

1040 **FIGURE S3**

1041
1042
1043
1044
1045
1046
1047
1048
1049
1050
1051
1052
1053
1054
1055
1056

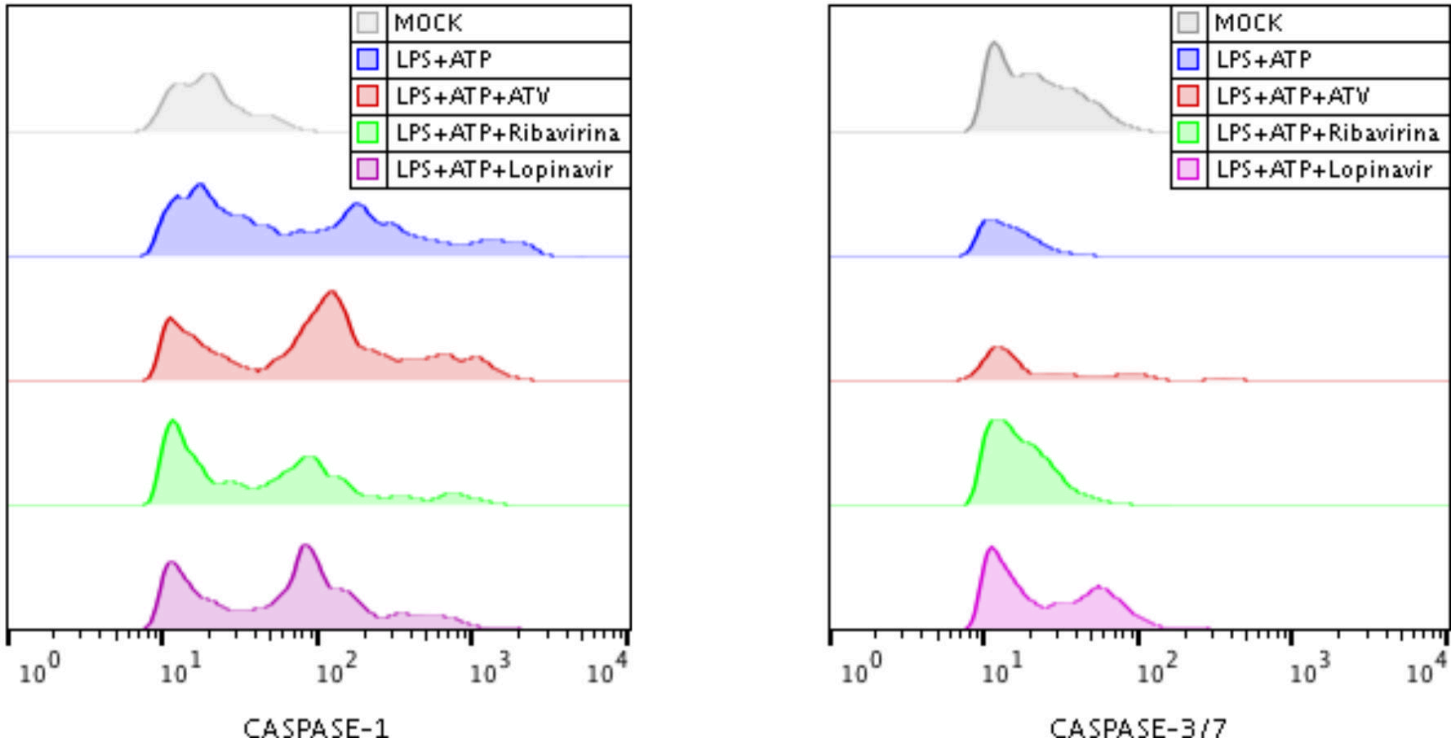

1057 **S3 Fig. Evaluation of anti-inflammatory activity of ATV, LPV and ribavirin in LPS-induced monocytes.** Human monocytes were stimulated
1058 with LPS (500ng/mL) for 23 h and after this time were stimulated with ATP (2 mM) for 1 h as a positive control group for the formation of
1059 inflammasomes and pyroptosis induction. Simultaneously, cells were treated with atazanavir – ATV (10 µM), LPV (10 µM) or ribavirin (10 µM)
1060 for 24 h. Monocytes were stained with FAM-YVAD-FLICA (blue) or FAM-FLICA (green) to determine the caspase-1 and caspase-3/7 activity
1061 and HLA-DR expression, respectively, and analyzed by flow cytometry. Histograms are representative of six independent experiments.

FIGURE S4

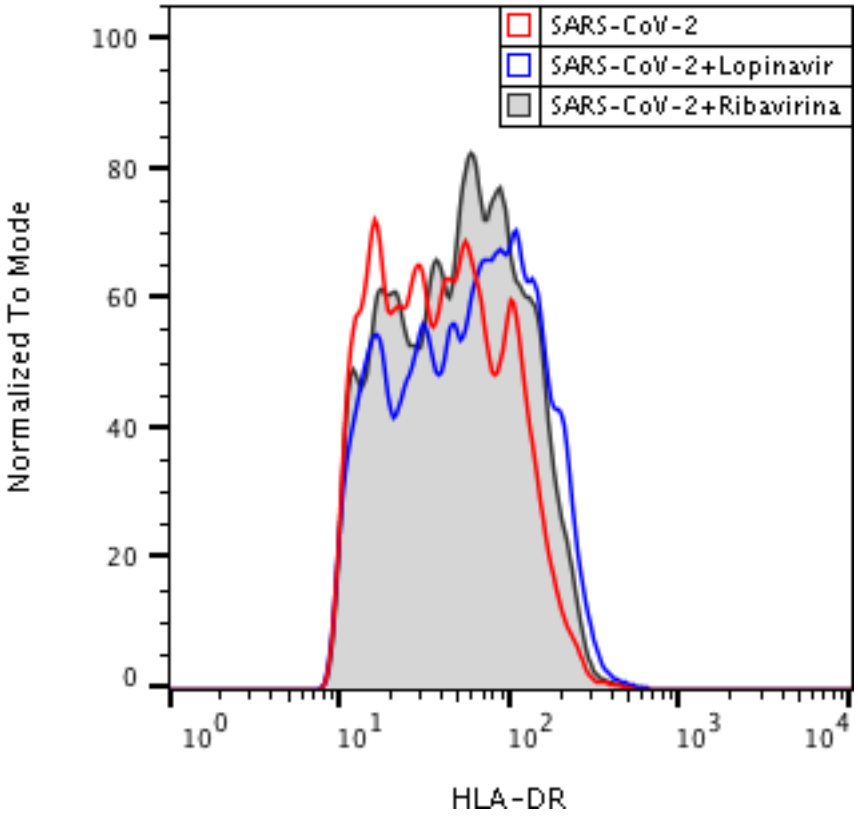

S4 Fig. Effects of LPV and ribavirin in preventing the SARS-CoV-2-related reduced expression of HLA-DR in monocytes. Human monocytes were infected with SARS-Cov-2 and treated with LPV (10 µM) or ribavirina (10 µM) for 24 h. Monocytes were stained with HLA-DR APC.H7 or IgG APC.H7 to determine the HLA-DR expression by flow cytometry. Histogram data are representative of six independent experiments.